Doping γ-Fe₂O₃ Nanoparticles with Mn(III) Suppresses the Transition to the α-Fe₂O₃ Structure

Jriuan Lai,[†,⊥] Kurikka V. P. M. Shafi,[†,⊥] Katja Loos,[†,⊥] Abraham Ulman,*[,†,⊥] Yongjae Lee,[‡]
Thomas Vogt,[‡] and Claude Estournès[§]

*Department of Chemical Engineering, Chemistry & Material Science, Polytechnic University, 6 Metrotech Center
Brooklyn, New York 11201, Physics Department, Brookhaven National Laboratory, P.O. Box 5000,
Upton, New York 11973-5000, and Institut de Physique et Chimie des Matériaux de Strasbourg Cedex, France*

Received April 1, 2003; E-mail: aulman@duke.poly.edu

Magnetic nanoparticles have applications in information storage,[1] color imaging,[2] magnetic refrigeration,[3] bioprocessing,[4] medical diagnosis,[5] controlled drug delivery,[6] and as ferrofluids.[7] Thus, developing a new synthetic route for magnetic nanoparticles and investigating their properties are of immense importance.

Ferrites, the transition metal oxides having a spinel structure, are technologically important because of their appealing magnetic and electrical properties. They are used in magnetic inks[8] and fluids,[9] as well as for the fabrication of magnetic cores of read/write heads for high-speed digital tapes or for disk recording.[10] Maghemite (γ-Fe₂O₃, the ferrimagnetic cubic form of iron(III) oxide) is also technologically important, as it is being used widely for the production of magnetic materials and catalysts. Because of the small coercivity of Fe₂O₃ nanoparticles, which arises from a negligible barrier in the hysteresis of the magnetization loop, they can also be used in magneto-optical devices.[11]

Various methods have been reported for the synthesis of metal oxide nanoparticles, such as wet chemical,[12] electrochemical,[13] pyrolysis,[14] and sol−gel reactions,[15] as well as chemical oxidation in micellar media[16] or polymers.[11] Recently, we have developed a new sonochemical route[17] for the preparation of coated γ-Fe₂O₃ nanoparticles.[18] Motivated by the potential of exploring the magnetic properties of particles in the nanosize regime, we have initiated systematic studies of oxides, ferrites, and garnets nanoparticles. Here we report on a mixed oxide system, γ-Fe₂O₃ nanoparticles doped with Mn(III), where the transition from the cubic to the more stable hexagonal α-Fe₂O₃ structure is suppressed.

Doped amorphous Fe₂O₃ nanoparticles were prepared by irradiating the mixture of amorphous Fe₂O₃ nanoparticles[18] and Mn₂(CO)₁₀ in 40 mL of decahydronaphthalene with a high-intensity ultrasonic horn under ambient conditions for 2 h. The resulting product was separated by centrifuge, washed thoroughly with dry pentane, and dried under vacuum. The as-prepared amorphous nanoparticles were then crystallized in a tube furnace under air.

Magnetic data of the nanoparticle samples were obtained with a Princeton Applied Research vibrating sample magnetometer, model 155 (VSM), and a Quantum Design SQUID MPMS-XL (AC and DC modes and maximum static field of 5 T).

Powder XRD was done using a Philips diffractometer (Cu Kα radiation, $\lambda = 1.5418$ Å), with a 0.008° resolution in 2θ. The measurement time was 2.5 h, and the 2θ range was from 15° to 85°. Initial synchrotron X-ray powder diffraction experiments were performed at the beamline X7A of the National Synchrotron Light Source (NSLS) at Brookhaven National Laboratory using a linear
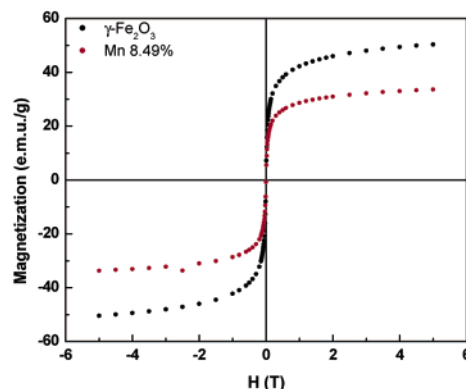
Figure 1. Magnetization curve of γ-Fe₂O₃ and γ-Fe₂O₃ doped with 8.5% Mn(III) at 295 K.

position-sensitive detector gating electronically on the Kr-escape peak.[19] See Supporting Information for details.

When amorphous Fe₂O₃ is heated at 300 °C for 3 h, ferrimagnetic γ-Fe₂O₃ is observed as the sole product.[18] On the other hand, when the temperature is raised to 500 °C, one observes only antiferromagnetic α-Fe₂O₃ as the product. Therefore, we were surprised to find that, upon doping with 8.5 wt % Mn(III), the amorphous nanoparticles crystallized to mainly the γ-Fe₂O₃ matrix after heating at 500 °C for 3 h (Figure 1, Supporting Information), with some peaks showing a strained α-phase. Moreover, the annealed nanoparticles showed superparamagnetic behavior (Figure 1). The magnetic measurements also show that the doping of Mn(III) reduces the maximum magnetization. The question was if the structure at 500 °C is the α- or γ-Fe₂O₃. In other words, can it be that at 500 °C the structure is α-Fe₂O₃-"like", and upon cooling transforms to the γ-Fe₂O₃ structure? We therefore heated 8.5% Mn-(III)-doped amorphous Fe₂O₃ nanoparticles at 500 °C for 3 h and quenched them in liquid nitrogen. XRD shows a highly strained α-Fe₂O₃ structure (Figure 3, Supporting Information), whereas the normally cooled (10 °C/min) sample resulted in a largely γ-Fe₂O₃ phase (Figure 1, Supporting Information). This suggests that the γ-to-α transition is not complete, even at high temperatures, and Mn(III) doping effectively suppresses the transition to the thermodynamically stable phase. Recall that γ-Fe₂O₃ is a metastable form, and the presence of Mn(III) ions stabilizes this form since the activation energy is substantially increased by Mn(III) doping.

The electron diffraction patterns of α-Fe₂O₃ (Figure 2a, Supporting Information) and γ-Fe₂O₃ (Figure 2b, Supporting Information) from TEM show spotty rings, which is the result of polycrystallinity . Due to the sintering, the bright-field images show the aggregation of annealed nanoparticles.

To further investigate this phase transition, we have recorded synchrotron X-ray diffraction patterns as a function of temperature,
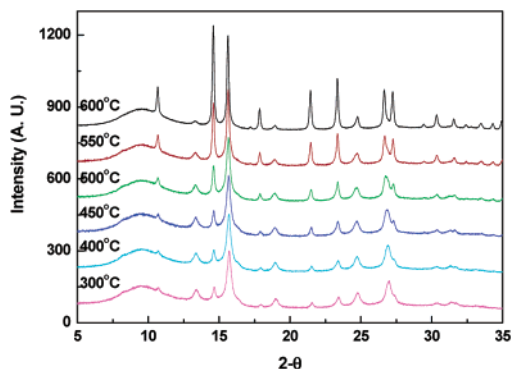
Figure 2. Temperature-dependent synchrotron powder X-ray diffraction of preannealed 8.5% Mn(III)-doped Fe_2O_3 nanopartciles.
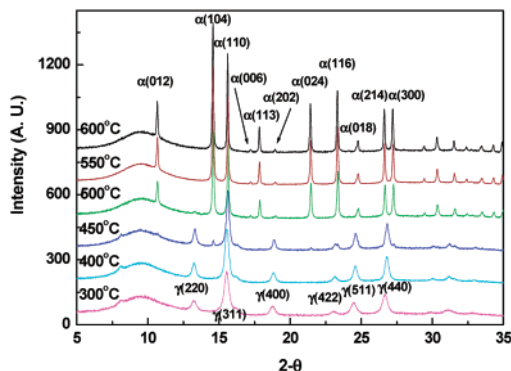

Figure 3. Temperature-dependent synchrotron powder X-ray diffraction of 5% Mn(III)-doped amorphous Fe_2O_3 nanopartciles.

starting from crystallized (500 °C, 3 h) 8.5% Mn(III)-doped γ-Fe_2O_3 nanoparticles (as in Figure 1, Supporting Information). A powdered sample (~0.003 g) was loaded into a 0.5-mm quartz capillary which was not sealed. A horseshoe-shaped heater was placed close to the sample position. A continuous heating rate of 8 °C/min was used. The imaging plate was exposed for 50 s for each frame without slits, and a readout time of ~110 s was used for scanning and storing. The wavelength of 0.9198 Å, sample-to-detector distance, zero point, and the IP tilt were determined using a LaB6 standard (NIST SRM 660a) prior to the experiment. The temperature was calibrated using the known thermal expansion of an Ag standard. Data were integrated using the FIT2D suite of programs.

Our results indicated that the transformation from γ- to α-Fe_2O_3 begins at 300 °C and is essentially completed at 600 °C (Figure 2). Notice that, at 500 °C, the structure is mostly γ-Fe_2O_3. The structure described earlier for amorphous nanoparticles heated to 500 °C and subsequently quenched is obviously a metastable one, and should therefore be assigned as α^*-Fe_2O_3. Once the sample is heated to 650 °C, a stable α-Fe_2O_3 is formed that does not change after cooling to room temperature.

The important question of how much doping of Mn(III) suppresses the γ-to-α transition was addressed in preliminary experiments, which revealed that the critical lower limit is between 5 and 8.5% Mn(III) doping. Thus, when a sample of 5% Mn(III)-doped amorphous Fe_2O_3 nanoparticle was heated to 500 °C for 3 h, nanoparticles with the stable α-Fe_2O_3 structure were formed. A full study of the various Fe:Mn compositions is still underway.

In an attempt to better understand the γ- to α-Fe_2O_3 transition in this system, we have also obtained in situ synchrotron X-ray diffraction patterns of the reaction of amorphous 5% Mn(III)-doped Fe_2O_3 nanoparticles. Figure 3 shows patterns starting at 300 °C (those between 25 and 300 °C were omitted for clarity). The crystal structure starts to change at 450 °C, transforming to α-Fe_2O_3 at

500 °C. This result is in very good agreement with quenching experiments, where the XRD of the same nanoparticles heated to 450 °C and quenched into liquid nitrogen revealed a highly amorphous product (see Figure 4, Supporting Information).

In summary, we have established that, when 8.5% Mn(III)-doped Fe_2O_3 amorphous nanoparticles are heated at 500 °C for 3 h, γ-Fe_2O_3 is obtained rather than α-Fe_2O_3. Even preannealed samples require temperatures as high as 600 °C to completely convert to the α-phase, indicating a high activation energy for this process. On the other hand, heating amorphous 5% Mn(III)-doped Fe_2O_3 nanoparticles at 500 °C for 3 h results in a product with the α-Fe_2O_3 structure. The suppression of the γ- (cubic) to α-Fe_2O_3 (hexagonal) transition is due to the fact that, while Mn(III) has a cubic spinel phase (with more free volume), it does not transform into a hexagonal one, and therefore doping Fe_2O_3 with Mn(III) increases the activation energy for the transition to the more compact α-phase, which requires lattice contraction. Thus, above a critical concentration (between 5 and 8.5%), the transition needs temperatures higher than 600 °C to complete. Preliminary results show that the same suppression occurs in Co_2O_3-doped Fe_2O_3 nanoparticles. The 8.5% Mn(III)-doped γ-Fe_2O_3 displays superparamagnetic behavior at room temperature, suggesting that doping might be used to tailor the magnetic properties of nanoparticles.

Supporting Information Available: XRD of 8.5% Mn(III)-doped γ-Fe_2O_3, TEM images of α-Fe_2O_3 and γ-Fe_2O_3, detail synchrotron X-ray pattern of 5% Mn(III)-doped Fe_2O_3, and XRD of 5% Mn(III)-doped Fe_2O_3 with heating at 450 °C for 3 h (PDF). This material is available free of charge via the Internet at http://pubs.acs.org.

References

(1) Audram, A. G.; Huguenard, A. P. U.S. Patent 4,302,523, 1981.
(2) Ziolo, R. F. U.S. Patent 4,474,866, 1984.
(3) McMichael, R. D.; Shull, R. D.; Swartzendruber, L. J.; Bennett, L. H.; Watson, R. E. *J. Magn. Magn. Mater.* **1992**, *111*, 29.
(4) (a) Pope, N. M.; Alsop, R. C.; Chang, Y.-A.; Sonith, A. K. *J. Biomed. Mater. Res.* **1994**, *28*, 449. (b) Dyal, A.; Loos, K.; Noto, M.; Chang, S. W.; Spagnoli, C.; Shafi, K. V. P. M.; Ulman, A.; Cowman, M.; Gross, R. A. *J. Am. Chem. Soc.* **2003**, *125*, 1684.
(5) (a) Marchessault, R. H.; Richard, S.; Rioux, P. *Carbohydr. Res.* **1992**, *224*, 133. (b) Josephson, L.; Tsung, C. H.; Moore, A.; Weissleder, R. *Bioconjugate Chem.* **1999**, *10*, 186.
(6) Bhatnagar, S. P.; Rosensweig, R. E. *J. Magn. Magn. Mater.* **1995**, *149*.
(7) Rosensweig, R. E. *Ferrohydrodynamics*; MIT Press: Cambridge, 1985.
(8) Charles, S. W.; Popplewell, J. *Ferromagnetic Materials*; North-Holland: Amsterdam, 1980; Vol. 2.
(9) Mehtha, R. V.; Upadhyay, R. V.; Dasanacharya, B. A.; Goyal, P. S.; Rao, K. S. *J. Magn. Magn. Mater.* **1994**, *132*, 153.
(10) Kuliokowski, J.; Lenniewski, A. *J. Magn. Magn. Mater.* **1980**, *19*, 117.
(11) (a) Tang, B. Z.; Geng, Y.; Lam, J. W. Y.; Li, B.; Jing, X.; Wang, X.; Wang, F.; Pakhomov, A. B.; Zhang, X. X. *Chem. Mater.* **1999**, *11*, 1581. (b) Ziolo, R.; Giannelis, E. P.; Weinstein, B. A.; O'Horo, M. P.; Ganguly, B. N.; Mehrotra, V.; Russel, M. W.; Huffman, D. R. *Science* **1992**, *257*, 219.
(12) Ennas, G.; Marangiu, G.; Musinu, A.; Falqui, A.; Ballirano, P.; Caminiti, R. *J. Mater. Res.* **1999**, *14*, 1570.
(13) Pascal, C.; Pascal, J. L.; Favier, F.; Moubtassim, M. L. E.; Payen, C. *Chem. Mater.* **1999**, *11*, 141.
(14) Martinez, B.; Roig, A.; Molins, E.; Gonzalez-Carreno, T.; Serna, C. J. *J. Appl. Phys.* **1998**, *83*, 3256.
(15) Stober, W.; Fink, A.; Bohn, E. *J. Colloid Interface Sci.* **1968**, *26*, 62.
(16) Mounien, N.; Pileni, M. P. *Langmuir* **1997**, *13*, 3927.
(17) Suslick, K. S. *Science* **1990**, *247*, 1439.
(18) Shafi, K. V. P. M.; Ulman, A.; Dyal, A.; Yan, X.; Yang, N.-L.; Estournes, C.; Fournes, L.; Wattiaux, A.; White, H.; Rafailovich, M. *Chem. Mater.* **2002**, *14*, 1778.
(19) Smith, G. C. *Synch. Radiat. News* **1991**, *4*, 24.

JA035409D